Electro-optic control of atom-light interactions using Rydberg dark-state polaritons

M. G. Bason, A. K. Mohapatra, K. J. Weatherill, and C. S. Adams
Department of Physics, Durham University, Rochester Building, South Road, Durham DH1 3LE, England
(Received 17 September 2007; published 5 March 2008)

We demonstrate a multiphoton Rydberg dark resonance where a Λ system is coupled to a Rydberg state. This $\mathcal{N}$-type level scheme combines the ability to slow and store light pulses associated with long-lived ground-state superpositions with the strongly interacting character of Rydberg states. For the $nd_{5/2}$ Rydberg state in ^{87}Rb (with $n=26$ or 44) and a beam size of 1 mm, we observe a resonance linewidth of less than 100 kHz in a room-temperature atomic ensemble limited by transit-time broadening. The resonance is switchable with an electric field of order 1 V cm^{-1}. Applications in electro-optic switching and photonic phase gates are discussed.

DOI: 10.1103/PhysRevA.77.032305 PACS number(s): 03.67.Lx, 42.50.Gy, 32.80.Rm

I. INTRODUCTION

As photons are the most robust carriers of quantum information, there is considerable interest in developing single-photon sources, memories, and gates. The storage and retrieval of single photons using electromagnetically induced transparency (EIT) [1] have been demonstrated experimentally in both laser-cooled [2] and thermal atomic ensembles [3]. These experiments employ the dark-state polariton concept, where the photon is evolved into a single atomic spin excitation and back into a photon [4]. Dark-state polaritons involve three atomic energy levels, where two ground states are coupled via an excited state, forming a Λ system. The attractive feature of this level scheme is that the ground-state coherence is long lived, allowing photon storage times of the order of microseconds [2,3].

In principle, deterministic photon gates could be realized using a large nonlinearity at the single-photon level. Enhanced Kerr nonlinearities have been predicted in a medium displaying EIT [5], and have been studied in experiments on Bose-Einstein condensates [6] and cold atoms [7,8]. However, achieving a sufficiently large nonlinearity and matched group velocities for both photon pulses [9], without introducing pulse distortion, remains a problem. Recent theoretical work has focused on possible solutions based on frequency and intensity tuning [10], tight confinement of the light pulse [11], enhancing the interactions using Rydberg states [12], and double EIT [13]. Even if a large enough Kerr nonlinearity could be achieved, this may not be sufficient to realize high-fidelity quantum gates [14].

The strongly interacting character of Rydberg atoms [15] makes them particularly attractive for achieving entanglement, as discussed in the context of fast quantum gates for atoms [16,17]. Recently, we showed that it is possible to map the properties of Rydberg atoms, such as their high sensitivity to electric fields, onto a strong optical transition from the ground state using a ladder EIT scheme [18]. Theoretical calculations suggest that this level configuration could produce a cross-phase modulation of π for counterpropagating single-photon pulses in a dense ultracold atomic ensemble, providing a possible scheme for the realization of a photon gate [12].

In this paper, we demonstrate a multiphoton Rydberg dark resonance where a Λ system is coupled to a Rydberg state. This $\mathcal{N}$-type level scheme combines the attractive features of both ground-state dark-state polaritons [4] and Rydberg states, i.e., the ability to slow and store light pulses [2,3] and the long-range interactions associated with Rydberg atoms [15]. This long-range character of the Rydberg interaction means that the pulse distortion effects associated with the Kerr effect [14] could be substantially reduced [12]. In our experiment, we observe a Rydberg dark-resonance linewidth of less than 100 kHz in a room-temperature vapor, and show that the Rydberg dark resonance is switchable with an electric field of only 1 V cm^{-1}. Hence we demonstrate that the high polarizability of the Rydberg state can be mapped onto the ground-state coherence.

II. EXPERIMENT

The energy levels of ^{87}Rb used for the experimental demonstration of the multiphoton Rydberg dark resonance are shown in Fig. 1(a). A Λ system ($|1\rangle \rightarrow |2\rangle \rightarrow |3\rangle$) is formed by a weak probe beam with Rabi frequency Ω_{21} resonant with the $5s\ ^2S_{1/2}(F=1) \rightarrow 5p\ ^2P_{3/2}(F'=2)$ transition and a strong coupling beam with Rabi frequency Ω_{32} resonant with the

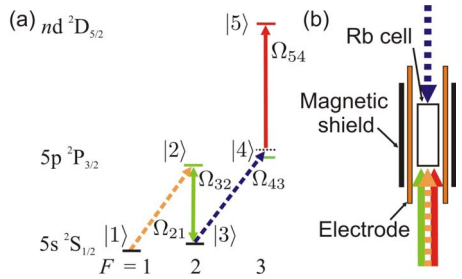

FIG. 1. (Color online) (a) Level scheme used for the experimental demonstration of a four-photon Rydberg dark resonance: The Λ system ($|1\rangle \rightarrow |2\rangle \rightarrow |3\rangle$) is coupled to a Rydberg state $|5\rangle$ using a two-photon transition via an intermediate state $|4\rangle$. The absorption or dispersion of the medium is detected on the transition $|1\rangle \rightarrow |2\rangle$ using a probe beam with Rabi frequency Ω_{21}. (b) Schematic of the experimental setup. The Λ-system beams [light solid (green) and dashed (orange)] copropagate with the second step of the Rydberg excitation [dark solid (red)]. The first step of the Rydberg excitation [dark dashed (purple)] is counterpropagating.

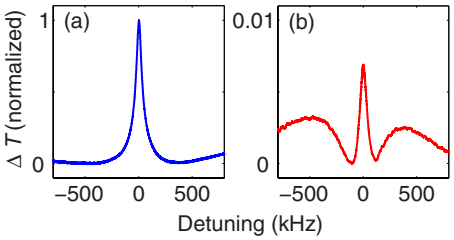

FIG. 2. (Color online) Experimental measurement of the change in transmission, ΔT, associated with (a) the Λ system $|1\rangle \rightarrow |2\rangle \rightarrow |3\rangle$ and (b) the Rydberg dark-resonance signal corresponding to the difference between the Λ-system resonance with Rydberg coupling ($n=26$) on and off. The Rydberg dark resonance (normalized relative to the Λ-system resonance) is measured using a lock-in amplifier and is over two orders of magnitude smaller than the Λ-system resonance.

$5s\ ^2S_{1/2}(F=2) \rightarrow 5p\ ^2P_{3/2}(F'=2)$ transition. The coupling beam is derived from a commercial 780.24 nm extended cavity diode laser that is locked directly to the $F=2 \rightarrow F'=2$ resonance using polarization spectroscopy [19]. A fraction of the coupling beam is passed through an electro-optic modulator (EOM) that adds sidebands at 6.8 GHz. A slave laser is injection locked onto the upper sideband to obtain the probe beam. A high spectral purity is obtained by using a double-injection scheme [20]. The probe beam can be scanned through the $F=1 \rightarrow F'=2$ resonance by changing the drive frequency of the EOM. The probe and coupling beams are combined on a polarization-beam-splitting cube and coupled into a polarization-maintaining single-mode fiber. The output of the fiber is collimated and propagates through a room-temperature Rb cell of length 75 mm as shown in Fig. 1(b). The probe and coupling beams have a waist of 1.3 mm ($1/e^2$ radius) and powers of 10 and 35 μW, respectively.

The Λ system is coupled to a Rydberg state using a two-photon excitation scheme as shown in Fig. 1(a). The first step is formed by a 780.24 nm beam resonant with the $5s\ ^2S_{1/2}(F=2) \rightarrow 5p\ ^2P_{3/2}(F'=3)$ transition that is derived by shifting the coupling light using two acousto-optic modulators (AOMs). The laser power incident on the cell is 40 μW. The second step is derived from a commercial frequency-doubled diode laser system (Toptica TA-SHG) at 480 nm that is resonant with the $5p\ ^2P_{3/2}(F'=3) \rightarrow nd\ ^2D_{5/2}(F'')$ transition (the nd-state hyperfine splitting is not resolved). The two-photon resonance is driven by counterpropagating beams in the vapor cell with the second step copropagating with the Λ-system beams as in Fig. 1(b). The 480 nm beam has a power of 140 mW and a waist of 0.8 mm ($1/e^2$ radius). The waist size is a trade-off between mode matching with the 780 nm beams and achieving a high Rabi frequency. The Rb vapor cell is placed between two copper bar electrodes and inside a single-layer magnetic shield. The 480 nm laser is frequency stabilized using a ladder-system Rydberg EIT signal [18] in a second Rb vapor cell. From the EIT error signal we estimate the linewidth of the 480 nm laser to be $\sim$150 kHz.

The spectrum corresponding to the Λ-system resonance is shown in Fig. 2(a). The linewidth of $\sim$70 kHz is limited mainly by transit-time broadening. To isolate the effect of the Rydberg coupling on the Λ system, we modulate the amplitude of the 480 nm laser at 35 kHz and monitor the probe signal using a lock-in amplifier. The lock-in signal, which corresponds to the change in the Λ resonance when the Rydberg coupling is switched on and off, is shown in Fig. 2(b). This signal disappears when any one of the four beams involved is blocked.

III. DISCUSSION

To understand the shape of the observed Rydberg dark-resonance signal and establish how the effect may be optimized in both thermal and ultracold atomic ensembles we have solved the optical Bloch equations for the five-level system. The five-level Hamiltonian may be written as

$$H = \frac{1}{2}\begin{pmatrix} \Delta_{21} & \Omega_{21} & 0 & 0 & 0 \\ \Omega_{21} & \Delta_{32}-k_1 v & \Omega_{32} & 0 & 0 \\ 0 & \Omega_{32} & 0 & \Omega_{43} & 0 \\ 0 & 0 & \Omega_{43} & \Delta_{43}+k_1 v & \Omega_{54} \\ 0 & 0 & 0 & \Omega_{54} & \Delta_{54}+k' v \end{pmatrix},$$

where the labels 1–5 refer to the states $5s\ ^2S_{1/2}(F=1)$, $5p\ ^2P_{3/2}(F'=2)$, $5s\ ^2S_{1/2}(F=2)$, $5p\ ^2P_{3/2}(F'=3)$, and $44d\ ^2D_{5/2}$, respectively, as in Fig. 1(a), Δ_{ij} and Ω_{ij} are the detuning and Rabi frequency between states i and j, k_1 and k_2 are the wave vectors of the 780 and 480 nm beams, $k'=k_1-k_2$, and v is the atomic velocity. The population in state i and coherence involving state i decay at rates γ_i and $\gamma_i/2$, respectively. Note that this is not a complete description of the experiment as the hyperfine splitting of the $5p\ ^2P_{3/2}$ state is less than the Doppler broadening, so there are multiple contributions to both the Λ and two-photon Rydberg resonances. However, the model does give qualitative insight into the properties of the Rydberg dark resonance.

In Fig. 3 we plot the imaginary part of the coherence between states $|1\rangle$ and $|2\rangle$, which determines the probe absorption. The thin lines indicate the absorption for different velocity classes. The thick red lines indicates the absorption of the zero velocity class atoms. The thick black line indicates the total absorption obtained by summing over velocity. Figure 3(c) shows the difference between the cases where the 480 nm laser is on and off, and reproduces the shape of the observed Rydberg dark resonance seen in Fig. 2(b). The signal arises because the $|3\rangle \rightarrow |4\rangle$ transition suppresses the Λ-system EIT resonance, and the Rydberg coupling renders the $|3\rangle \rightarrow |4\rangle$ transition dark such that the Λ resonance is recovered. Consequently, the central peak of the Rydberg dark-resonance signal has the same width as the Λ resonance.

Figures 3(a) and 3(b) show that the narrow contribution to the Rydberg dark resonance is from the zero-velocity-class atoms, while the wings of the signal arise from low-velocity atoms. The limitation to the size of the Rydberg dark resonance is due to the velocity averaging from the room-temperature atomic vapor. The signal could be enhanced either by using an ultracold atomic sample or by adjusting the

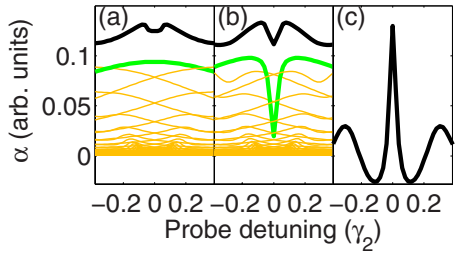

FIG. 3. (Color online) Absorption α (proportional to the imaginary part of the density matrix component σ_{21}) experienced by the probe beam as a function of detuning for a four-photon Rydberg dark resonance with the Rydberg coupling (a) off and (b) on. In (c) we show the difference between (a) and (b) ($\times 10$), which corresponds to the effect of coupling to the Rydberg state as observed in the experiment, Fig. 2(b). The specific parameters are $\Omega_{21}=0.02\gamma_2$, $\Omega_{32}=0.2\gamma_2$, $\Omega_{43}=0.8\gamma_2$, $\Delta_{43}=\Delta_{54}=0$, $\gamma_4=\gamma_2$, and $\gamma_5=0.01\gamma_2$. (a) $\Omega_{54}=0.0\gamma_2$ and (b) $\Omega_{54}=0.8\gamma_2$. The thin lines show velocities in the range $-10\gamma_2\lambda_1$ to $+10\gamma_2\lambda_1$ in steps of $0.5\gamma_2\lambda_1$. The thick light (green) lines indicates the absorption of the zero-velocity-class atoms. The thick black line indicates the total absorption obtained by summing over velocity. The curves for each velocity class are multiplied by 5 so that they can be plotted on the same scale as the sum.

beam intensities and detunings such that the multiphoton dark resonance becomes Doppler-free [21]. Both schemes will be investigated in future work. A Doppler-free configuration in a thermal ensemble would be particularly attractive due to the reduced experimental overhead involved in state preparation, resulting in much higher ''clock'' rate for a practical device. Solutions of the optical Bloch equations suggest that a Doppler-free resonance could be obtained using the $D1$ line and focusing the Rydberg laser into a short cell.

IV. ELECTRO-OPTIC EFFECT

The interesting feature of the $\mathcal{N}$-system Rydberg dark resonance is the ability to map the strongly interacting character of Rydberg atoms onto a ground-state coherence. To demonstrate this we show that, as a result of the Rydberg coupling, the Λ-system resonance for the zero velocity class has become highly sensitive to electric fields. We apply an ac electric field with frequency 20 MHz to the copper bar electrodes shown in Fig. 1(b), and measure the amplitude of the central peak of the Rydberg dark-resonance signal as a function of the rms field. An ac field is used to avoid the effects of charge screening inside the cell [18]. The results for the $n=44d_{5/2}$ state are shown in Fig. 4. The Rydberg dark resonance is suppressed with a field of the order of 1 V cm^{-1}. The shape of the curve can be explained by the electric field dependence of the $44d\ ^2D_{5/2}$ state, which splits into three components with the $|m_J|=5/2$ component shifting out of resonance at a lower field (of order 0.1 V cm^{-1}) and the other two components shifting out of resonance at 0.9 V cm^{-1} [18]. As the polarization scales as the seventh power of the principal quantum number, n^7, an even higher sensitivity can be expected for Rydberg states with larger n.

The results of Fig. 4 show that the polarizability of the Rydberg state is mapped onto the ground-state superposition.

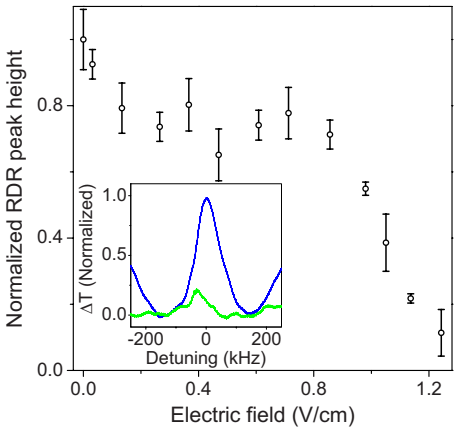

FIG. 4. (Color online) Electric field dependence of the Rydberg dark resonance (RDR) amplitude for $n=44$. The RDR signals at 0 V cm^{-1} [light (green)] and 1.1 V cm^{-1} [dark (blue)] are shown inset. Note that the relative height of the central peak and the wings is smaller for $n=44$ than $n=26$, Fig. 2(b), due to the lower value of Ω_{54}.

This opens the way to a number of interesting applications. First, one could use a dc applied electric field to switch the properties of the medium. Or one could exploit the Rydberg-Rydberg interactions [22] that give rise to the dipole blockade mechanism [23–27] to modify the medium from absorbing with a superluminal group velocity for single excitation to transparent with a slow group velocity for multiple excitations, resulting in a large nonlinearity at the single-photon level. The advantage of the $\mathcal{N}$-type system is that the photon pulse can be written into the medium and subsequently one induces the interaction via the Rydberg coupling, so the interaction is decoupled from the intensity of the pulse, thereby reducing the problem of pulse distortion highlighted in the context of single-photon Kerr nonlinearity [14]. Recent work by Friedler *et al.* [12] suggests that the interaction is spatially homogeneous.

V. CONCLUSIONS

In summary, we have demonstrated a four-photon Rydberg dark resonance with a linewidth of less than 100 kHz limited mainly by transit-time broadening. We show that resonance can be suppressed by applying an electric field of only 1 V cm^{-1}, and thereby demonstrate that the strongly interacting properties of Rydberg states can be mapped onto the ground-state coherence. This $\mathcal{N}$-system resonance involving a polarizable dark state could be enhanced using ultracold atoms or a Doppler-free scheme, and has considerable potential for electro-optic control of light propagation and photonic phase gates.

ACKNOWLEDGMENTS

We are grateful to M. P. A. Jones, K.-P. Marzlin, and P. F. Griffin for stimulating discussions. We thank the EPSRC for financial support.

[1] K.-J. Boller, A. Imamoğlu, and S. E. Harris, Phys. Rev. Lett. **66**, 2593 (1991); A. Kasapi, M. Jain, G. Y. Yin, and S. E. Harris, *ibid.* **74**, 2447 (1995).
[2] T. Chanelière, D. N. Matsukevich, S. D. Jenkins, S.-Y. Lan, T. A. B. Kennedy, and A. Kuzmich, Nature (London) **438**, 833 (2005).
[3] M. D. Eisaman, A. André, F. Massou, M. Fleischhauer, A. S. Zibrov, and M. D. Lukin, Nature (London) **438**, 837 (2005).
[4] M. Fleischhauer and M. D. Lukin, Phys. Rev. Lett. **84**, 5094 (2000).
[5] H. Schmidt and A. Imamoğlu, Opt. Lett. **21**, 1936 (1996).
[6] L. V. Hau, S. E. Harris, Z. Dutton, and C. H. Behroozi, Nature (London) **397**, 594 (1999).
[7] H. Kang and Y. Zhu, Phys. Rev. Lett. **91**, 093601 (2003).
[8] Y.-F. Chen, C.-Y. Wang, S.-H. Wang, and I. A. Yu, Phys. Rev. Lett. **96**, 043603 (2006).
[9] M. D. Lukin and A. Imamoğlu, Phys. Rev. Lett. **84**, 1419 (2000).
[10] C. Ottaviani, D. Vitali, M. Artoni, F. Cataliotti, and P. Tombesi, Phys. Rev. Lett. **90**, 197902 (2003).
[11] A. André, M. Bajcsy, A. S. Zibrov, and M. D. Lukin, Phys. Rev. Lett. **94**, 063902 (2005).
[12] I. Friedler, D. Petrosyan, M. Fleischhauer, and G. Kurizki, Phys. Rev. A **72**, 043803 (2005).
[13] Z.-B. Wang, K.-P. Marzlin, and B. C. Sanders, Phys. Rev. Lett. **97**, 063901 (2006).
[14] J. H. Shapiro, Phys. Rev. A **73**, 062305 (2006).
[15] T. F. Gallagher, *Rydberg Atoms* (Cambridge University Press, Cambridge, U.K., 1994).
[16] D. Jaksch, J. I. Cirac, P. Zoller, S. L. Rolston, R. Côté, and M. D. Lukin, Phys. Rev. Lett. **85**, 2208 (2000).
[17] M. D. Lukin, M. Fleischhauer, R. Côté, L. M. Duan, D. Jaksch, J. I. Cirac, and P. Zoller, Phys. Rev. Lett. **87**, 037901 (2001).
[18] A. K. Mohapatra, T. R. Jackson, and C. S. Adams, Phys. Rev. Lett. **98**, 113003 (2007).
[19] C. P. Pearman, C. S. Adams, S. G. Cox, P. F. Griffin, D. A. Smith, and I. G. Hughes, J. Phys. B **35**, 5141 (2002).
[20] M. G. Bason, A. K. Mohapatra, K. J. Weatherill, and C. S. Adams (unpublished).
[21] C. Y. Ye, A. S. Zibrov, Yu. V. Rostovtsev, and M. O. Scully, Phys. Rev. A **65**, 043805 (2002).
[22] J. M. Raimond, G. Vitrant, and S. Haroche, J. Phys. B **14**, L655 (1981).
[23] K. Singer, M. Reetz-Lamour, T. Amthor, L. G. Marcassa, and M. Weidemüller, Phys. Rev. Lett. **93**, 163001 (2004).
[24] D. Tong, S. M. Farooqi, J. Stanojevic, S. Krishnan, Y. P. Zhang, R. Côté, E. E. Eyler, and P. L. Gould, Phys. Rev. Lett. **93**, 063001 (2004).
[25] T. Cubel Liebisch, A. Reinhard, P. R. Berman, and G. Raithel, Phys. Rev. Lett. **95**, 253002 (2005).
[26] T. Vogt, M. Viteau, J. Zhao, A. Chotia, D. Comparat, and P. Pillet, Phys. Rev. Lett. **97**, 083003 (2006).
[27] R. Heidemann, U. Raitzsch, V. Bendkowsky, B. Butscher, R. Löw, L. Santos, and T. Pfau, Phys. Rev. Lett. **99**, 163601 (2007).